Shear viscosity and diffusion in liquid MgSiO$_3$: Transport properties and implications for terrestrial planet magma oceans

DEAN NEVINS,[1,*] FRANK J. SPERA,[1] AND MARK S. GHIORSO[2]

[1]Department of Earth Science, University of California, Santa Barbara, California 93106, U.S.A.
[2]OFM Research-West, 7336 24th Avenue NE, Seattle, Washington 98115, U.S.A.

ABSTRACT

Molecular dynamics simulations using a pair-wise additive potential are implemented to investigate self-diffusion (Mg, Si, and O) and shear viscosity of liquid MgSiO$_3$ in the density-temperature-pressure range 2350–5300 kg/m^3, 2500–5000 K, and 0–140 GPa, respectively. Self-diffusivity and shear viscosity are described by modified Arrhenian expressions, which feature a pressure-dependent activation volume. Activation energies for self-diffusion (Mg, Si, and O) and viscous flow are 99.6, 109.3, 97.4, and 95.3 kJ/mol, respectively; evidently oxygen mobility dominates liquid dynamics. Activation volumes for self-diffusion and shear viscosity at low (2–5 GPa) pressure are ~1 cm^3/mol with self-diffusion decreasing and shear viscosity increasing as pressure increases although there is a small interval near zero pressure within which diffusivity increases slightly with increasing pressure. Shear viscosity increases by a factor of 75 along the 3000 K isotherm from the top of the mantle to the core-mantle boundary. Along the 3000 K isentrope relevant to terrestrial magma ocean convection, shear viscosity increases by about a factor of three. The equivalence conditions between the Stokes-Einstein and Eyring transport models are derived. The Eyring model provides information on the size of the activated complex associated with viscous flow across the range in pressures relevant to the Earth's mantle and suggests that the number of atoms in the activated complex associated with shear flow decreases from ~8 atoms at low pressure to ~4 atoms at high pressure at 4500 K.

Keywords: Geochemical modeling, high-pressure behavior, mantle processes, composition of the mantle, transport properties, MgSiO$_3$

INTRODUCTION

An understanding of the structure, equation of state (EOS), and transport properties of molten silicates at high temperature (T) and pressure (P) is central to many aspects of planetary dynamics. For example, understanding the cooling and crystallization of Earth's early magma ocean requires knowledge of the thermodynamic and transport properties of MgO-rich silicate liquids at P and T in the range 0–135 GPa and 2500–6000 K, respectively. Even higher pressures are important in modeling "Super-Earth" terrestrial exoplanets (Valencia et al. 2007) that may go through an early magma ocean stage. The state of the mantle following magma ocean solidification has significant bearing on the start of subduction, the plate tectonic cycle, the subsequent evolution of the lithosphere, continental and oceanic crust, hydrosphere and atmosphere (Anderson 2007). Seismic tomography has revealed heterogeneities in the lower mantle that may be the remnants of lower mantle chemical heterogeneity associated with the solidification of Earth's early magma ocean (e.g., Garnero and McNamara 2008; Boyet and Carlson 2005; Bennett et al. 2007). The possible presence today of pockets of melt along the Earth's core-mantle boundary has also been suggested (Lay et al. 2004). Knowledge of the shear viscosity of molten MgSiO$_3$, a reasonable analog composition for the

Hadean magma ocean on Earth, is useful in studying these and other geodynamical problems involving molten silicates. In this study, we use the molecular dynamics method with the effective pair-potential from Oganov et al. (2000) to compute the shear viscosity of liquid MgSiO$_3$ by Green-Kubo theory (Hansen and McDonald 2006) and the self-diffusivity of Mg, Si, and O at elevated T and P. We show that the P-T variation of shear viscosity is well-fit by a modified Arrhenian expression featuring a pressure-dependent activation volume for viscous flow and that at high temperature, the shear viscosity increases by a factor of ~60 along high-temperature isotherms. The viscosity expression can be used with the MD-derived EOS to generate values along high-temperature isentropes relevant to terrestrial magma ocean convection. Viscosity increases by about a factor of three across the pressure range of the mantle along the isentrope. Finally, we show the relationship between the Stokes-Einstein and Eyring relations that connect self-diffusion to shear viscosity and use the latter model to estimate the size of the activated complex associated with viscous flow in liquid MgSiO$_3$.

THEORY AND EXPERIMENTAL METHODS

MD simulations were run with 8000 particles using the large-scale atomic/molecular massively parallel simulator (LAMMPS) (Plimpton 1995) modified for geochemical applications. Details of the algorithm and simulation methodology may be found elsewhere (Nevins and Spera 2007; Nevins 2009). The interatomic potential employed accounts for Coulomb forces, Born electron repulsion, and

---

* E-mail: dean@nevins.org

van der Waals attractive forces:

$$\Phi_{ij}(r_{ij}) = \frac{q_i q_j e^2}{4\pi \varepsilon_o r_{ij}} + A_{ij}\exp\left(-\frac{r_{ij}}{B_{ij}}\right) - \frac{C_{ij}}{r_{ij}^6} \tag{1}$$

where $\Phi_{ij}(r_{ij})$ is the interatomic potential; ε_o is the permittivity of free space; r_{ij} is the distance between atoms i and j; q_i, and q_j are the charges of the ith and j^{th} atoms, respectively; and A_{ij}, B_{ij}, and C_{ij} are parameters quantifying the energetics that were derived by Oganov et al. (2000), using results from GULP (Gale 1997). The potential parameters (Table 1) ignore all cation-cation interactions and the C_{ij} term is zero for all atom pairs except O-O. For each simulation run, initial conditions were set using the skew-start method of Refson (2001) and velocity scaling to maintain the temperature at 10 000 K for 20 picoseconds (ps) during thermal equilibration. The time step was 1 femtosecond (fs) in all calculations. After stabilizing at 10 000 K, velocity scaling was released and the system was run for 2 ps before cooling the material at a rate of 100 K/ps. The cooled material was run with no restraints for 2 ps to ensure temperature stability. Once thermal equilibration was demonstrated, 50 ps production runs were completed. A total of 80 MD simulations of 50 ps duration were performed for density (ρ) and T in the range 2350–5300 kg/m³ and 2500–5000 K, respectively. Twenty-seven additional simulations of 2 nanosecond (ns) duration were performed for viscosity computations for P in the range 0–120 GPa at 3500, 4000, and 4500 K.

It is instructive to compare the EOS from our work to the first-principles molecular dynamics (FPMD) results of Stixrude and Karki (2005) and Wan et al. (2007). This comparison is shown in Figure 1 in the pressure-volume (P-V) plane along the 3500 K isotherm. The pair-potential used here compares quite favorably with the FPMD potentials throughout the pressure range of interest and at other temperatures (not shown). A different potential used by Lacks et al. (2007) combines the potential of van Beest et al. (1990) for silica with Mg-O interaction parameters derived by fitting to the experimental P-V data of Speziale et al. (2001). We have compared our work with Lacks et al. (2007) and Stixrude and Karki (2005) at 3000 K in Figure 2. Our work compares favorably to both potentials in this case as well. One advantage of the potential used in this work is that the EOS derived from it by MD simulation is consistent with the experimentally determined Clapeyron slope of the fusion curve for MgSiO₃ (Ghiorso 2004). None of the potentials used by other investigators satisfies this experimental constraint.

Self-diffusivities for Mg, Si, and O were computed using the Einstein relation connecting the mean squared displacement (MSD) in the asymptotic limit of long times to the self-diffusivity (D):

$$D = \frac{1}{6N}\lim_{t\to\infty}\frac{d}{dt}\left\langle\sum_i^N\left[r_i(t) - r_i(0)\right]^2\right\rangle \tag{2}$$

where N is the number of particles, t is time, $r_i(t)$ is the position of a particle at time t, and the brackets refer to an average over time origins. The MSD was computed over the full 50 ps production run, which allowed for robust self-diffusivity statistics (Haile 1992).

The shear viscosity was computed using the Green-Kubo (GK) expression during post-processing. The Green-Kubo expression for the shear viscosity is given by integration of the stress (pressure) autocorrelation function,

$$\eta = \frac{V}{3kT}\int_0^\infty\left\langle\sum_{x<y}P_{xy}(t)P_{xy}(0)\right\rangle dt \tag{3}$$

In particular, the shear viscosity is computed according to Equation 3 where η is the shear viscosity, V is the system volume, and P_{xy} refers to the xy component of the stress. As was the case with Equation 2, the brackets indicate an averaging over time origins. In addition to P_{xy}, other off-diagonal components of the stress tensor (P_{xz}, P_{yz}) as well as the first differences ($P_{xx} - P_{yy}$) and ($P_{yy} - P_{zz}$) are used to compute independent estimates of the shear viscosity. The reported viscosity is an average of all five independent estimates following the method developed by Nevins and Spera (2007). The GK formulation utilizes a single summation that consolidates the contributions of all the atoms into a single autocorrelation function thereby allowing the formulation to be used with molecular dynamics simulations. Alternative formulations based on particle displacement require translational invariance, an assumption violated in MD simulations utilizing periodic boundary conditions (Haile 1992). The parameters used to optimize the viscosity computation include a simulation duration (t_D) of 2 ns, a window width (t_W) of 2, 10, or 12 ps, and a time interval between the start of successive time windows (t_S) of 10 fs.

TABLE 1. Potential interaction parameters used in MD simulations from Oganov et al. (2000)

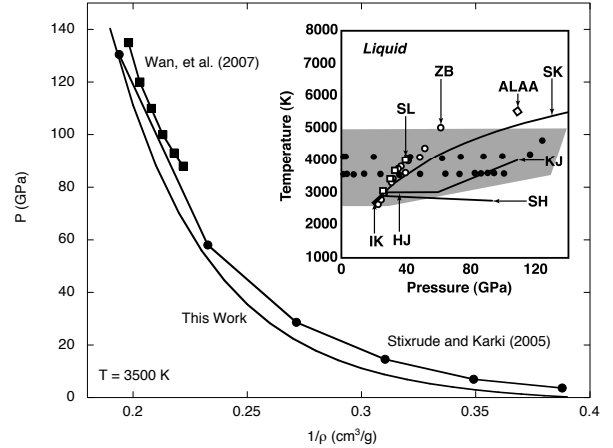| i	j	A_{ij} (kJ/mol)	B_{ij} (nm)	C_{ij} (nm⁶/mol)
Mg	Mg	0	0	0
Mg	Si	0	0	0
Mg	O	1.004808×10^5	0.02866	0
Si	Si	0	0	0
Si	O	1.097039×10^5	0.02827	0
O	O	1.952624×10^5	0.02674	3.189199×10^{-4}

FIGURE 1. Comparison of EOS data for MgSiO₃ liquid at 3500 K. Filled circles show interpolated 3500 K results of Stixrude and Karki (2005). The filled squares are the 3500 K data of Wan et al. (2007) and the smooth curve is this work. The inset depicts the melting curve modified from Stixrude and Karki (2005) with the location in P-T space of 25 viscosity values given by the filled circles; shaded area represents P-T coverage for 80 EOS runs conducted as part of this study. Estimate of the fusion curve referenced in the figure are: ALAA (Akins et al. 2004), HJ (Heinz and Jeanloz 1987), IK (Ito and Katsura 1992), KJ (Knittle and Jeanloz 1989), SH (Sweeney and Heinz 1993), SK (Stixrude and Karki 2005), SL (Shen and Lazor 1995), and ZB (Zerr et al. 1998).
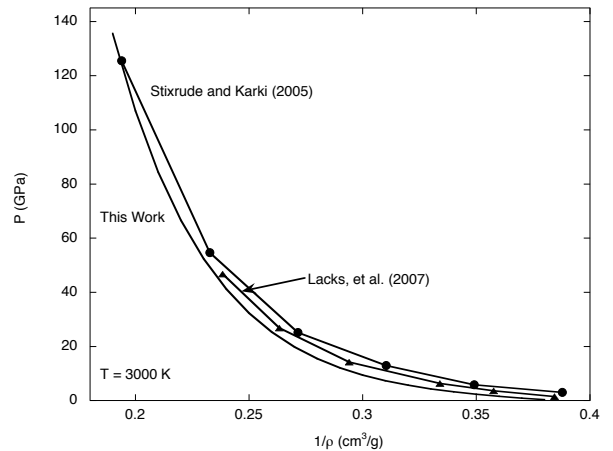

FIGURE 2. Comparison of EOS data for MgSiO₃ liquid at 3000 K. The filled circles are the data of Stixrude and Karki (2005) and the filled triangles are the data of Lacks et al. (2007). The smooth curve is this work.

RESULTS

Self-diffusivities (D) of Mg, O, and Si were determined at all state points. In Figure 3, results at 3553 ± 45 K for pressure in the range 0–98 GPa are shown. The solid curves give the calculated fit (parameters in Table 2) derived from the MD values. The fit expression is a modified Arrhenian relation that accounts for the pressure dependence of the activation volume for diffusion:

$$D = D_0 \exp\left(\frac{-(E_D^* + P[V_{D_0}^* + PV_{D_1}^*])}{RT}\right) \tag{4}$$

where E_D^* is the activation energy for diffusion, and $V_{D_0}^*$ and $V_{D_1}^*$ are the activation volume parameters. Other fit forms, such as the Vogel-Tammann-Fulcher (VTF) model suitably modified to incorporate the effects of pressure, provided a significantly worse fit of the raw MD data compared to the modified Arrhenian expression of Equation 4. The self-diffusivities of Mg, Si, and O at 88 GPa and 3500 K are 5.4×10^{-10}, 4.4×10^{-10}, and 1.3×10^{-9} m²/s, respectively. This compares with 1.14×10^{-9} m²/s given by Wan et al. (2007) presumably representing an average over all atom types suitably weighted although this was not specified in their paper. The self-diffusivity of all atoms decreases as P increases along an isotherm except for a very small region near zero pressure for oxygen (see inset Fig. 3), a weak example of
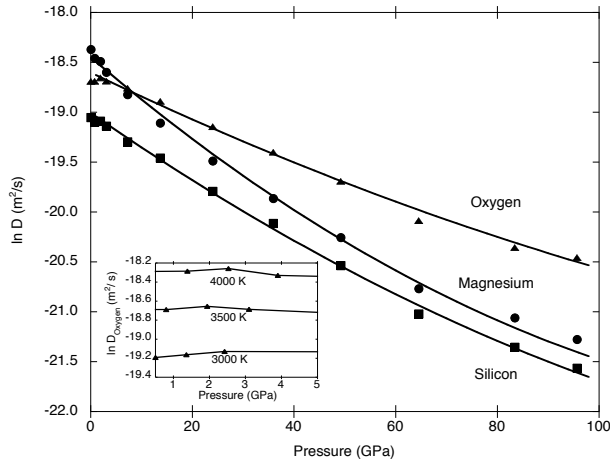
so-called anomalous diffusion as noted by Kubicki and Lasaga (1991). Si is the least mobile atom throughout the P-T range of the simulations. Oxygen is generally the most mobile except at $P < \sim 3$ GPa where the self-diffusivity of Mg is greatest. The activation volume at zero pressure ($V_{D_0}^*$ in Table 2) varies by a factor of two from 0.7 cm³/mol for O to 1.3 cm³/mol for Mg. Activation energies vary from 110 kJ/mol for Si to 97 kJ/mol for O. The modified Arrhenian expression provides an excellent fit for self-diffusivities in the range of P and T conditions studied here. Our self-diffusivities can be compared to those of Lacks et al. (2007) by evaluating Equation 4 at the P-T values of Lacks et al. (2007). This gives the comparison shown in Table 3. The diffusivities of silicon and oxygen compare well at low to intermediate pressures but deviate considerably for pressure greater than about 25 GPa. The potential we have used was derived by Oganov et al. (2000) specifically for high-pressure applications (e.g., the perovskite to post-perovskite phase transition) and that may explain the observed behavior. The diffusivity for magnesium does not agree well with Lacks et al. (2007) initially but it does improve with increasing pressure. We speculate that this might be the result of the Lacks et al. (2007) potential using the high-pressure crystalline data of Speziale et al. (2001) to obtain the magnesium-oxygen parameters. Because no laboratory measurements of Mg, Si, and O self-diffusivity are available at these P-T conditions it is impossible to know which values more accurately capture the behavior of the real material.

The shear viscosity (η) of MgSiO₃ from 0–103 GPa at 3552 ± 60 K, 0–116 GPa at 4042 ± 49 K, and at 120 GPa at 4500 ± 32 K calculated by the Green-Kubo method is shown in Figure 4. Plotted points represent the raw MD values, whereas the curves represent fits to the modified Arrhenian relationship:

$$\eta = \eta_0 \exp\left(\frac{E_\eta^* + P[V_{\eta_0}^* + PV_{\eta_1}^*]}{RT}\right) \tag{5}$$

where E_η^* is the activation energy for viscous flow, and the activation volume for viscous flow is solely a function of pressure according to $V_\eta^*(P) = V_{\eta_0}^* + PV_{\eta_1}^*$. Note that Equation 5 is identical in form to Equation 4. Calculated fit parameters are given in Table 2. Viscosity increases by a factor of 40 at 3500 K from 1 bar to 134 GPa, the pressure at the core-mantle boundary on Earth. At 3000 K, the ratio is 73, and at 4000 K the ratio is 25. The absolute value of the shear viscosity at 4000 K and 134 GPa is 0.074 Pa s; at 10^{-4} GPa (1 bar) and 4000 K the viscosity is estimated to be 0.0029 Pa s. The activation energy for viscous flow, 95 kJ/mol, is practically identical to the activation energy for oxygen self-diffusion (97 kJ/mol) and suggests that oxygen

FIGURE 3. Self-diffusion of O, Si, and Mg in MgSiO₃ liquid. The filled shapes represent the diffusion of oxygen (triangles), magnesium (circles), and silicon (squares). The solid lines are the predictions based on the parameters in Table 2. The inset shows a slight "anomalous diffusion" for oxygen at 3000, 3500, and 4000 K.

TABLE 2. Activation energies and volumes computed by regression of MD-derived diffusion and viscosity values

	D_0 (m²/s) or η_0 (Pa s)	E^*(kJ/mol)	V_0^*(cm³/mol)	V_1^*(cm³/mol GPa)	R^2
Mg	1.913×10^{-8}	99.642	1.283	-3.904×10^{-3}	0.98
Si	1.041×10^{-8}	109.285	1.045	-2.544×10^{-3}	0.98
O	1.541×10^{-8}	97.388	0.721	-1.424×10^{-3}	0.99
η	4.023×10^{-3}	95.063	1.375	-4.219×10^{-3}	0.98

Notes: Numerical values for both E^* and V^* are given in rational units for comparison; in any calculations all quantities should be expressed in SI units. R^2 refers to the coefficient of determination.

TABLE 3. Predicted self-diffusion using Equation 4, the parameters from Table 2 and the temperature and pressure values from Table 1 in Lacks et al. (2007) at $T = 3000$ K

P (GPa)	$D_{Mg} \times 10^{10}$ (m²/s)	$D_{Si} \times 10^{10}$ (m²/s)	$D_O \times 10^{10}$ (m²/s)
1.54	48.74 (105.0)	26.71(20.7)	43.90 (30.9)
3.67	43.76 (99.9)	24.45 (25.6)	41.31 (34.7)
6.39	38.21(79.9)	21.88 (24.4)	38.24 (35.4)
14.30	26.09 (47.7)	15.97 (17.7)	30.72 (26.2)
26.90	14.80 (24.4)	9.93 (7.7)	21.99 (12.0)
46.80	6.69 (7.3)	5.0(1.8)	13.45 (2.53)

Note: Diffusivities from Lacks et al. (2007). MD study using based on a different potential are given in parentheses.
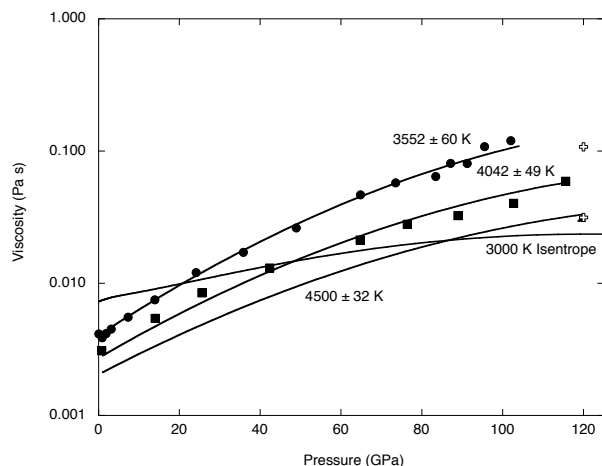
FIGURE 4. Viscosity of MgSiO$_3$ liquid. The circles and squares are MD-computed viscosity values at 3552 ± 60 and 4042 ± 49 K. The (partially obscured) solid triangle is a point at 4500 ± 32 K and 120 GPa. The curves represent the fit expression (Eq. 5 and Table 2). The two plus signs are the Wan et al. (2007) results at 4000 and 4500 K and 120 GPa.

activation sets the tempo for viscous flow. The zero-pressure activation volume for viscous flow of ~1.38 cm^3/mol is close to the zero-pressure activation volume for Mg self-diffusion (1.28 cm^3/mol) and about twice the value for oxygen self-diffusion (0.72 cm^3/mol). The activation volume for viscous flow decreases by ~0.004 cm^3/mol GPa and is similar to the absolute value of the comparable quantity for self-diffusion recorded in Table 2. The viscosity data shown in Figure 4 can be compared to two values reported in Wan et al. (2007) who used the generalized Debye-Stokes-Einstein formula derived by Zwanzig (1983) to relate self-diffusivity to shear viscosity. At 120 GPa and 4000 K, our predicted value for the shear viscosity is 0.065 Pa s compared to the range cited by Wan et al. (2007) of 0.083–0.114 Pa s. For 120 GPa and 4500 K, we find a value of 0.033 Pa s that compares very well to the value of 0.032 Pa s reported by Wan et al. (2007). It should be noted that Wan et al. (2007) did not determine D and η independently, but instead used the Debye-Stokes-Einstein relation and an estimate of the size of the diffusing "unit" to compute the shear viscosity. Below we use the independently computed D and η to determine, rather than assume, the characteristic size of the activated complex relevant to viscous flow and diffusive atom mobility.

DISCUSSION

We can quantitatively assess the increase of the shear viscosity in a terrestrial magma ocean by calculating the viscosity ratio across the pressure interval of the Earth's mantle (10^{-4} to 134 GPa) along the adiabat. The viscosity would increase by about a factor of 3–5 within the well-mixed interior depending on the precise adiabat. Boyet and Carlson (2005) suggest that the presence of a complementary enriched reservoir at the base of the mantle isolated since the Hadean would explain observed differences in ^{142}Nd/^{144}Nd between chondritic meteorites and terrestrial rocks. According to their proposal, this reservoir has never been sampled. Similarly, Bennett et al. (2007) proposed

models of early earth mantle dynamics to explain isotope systematics requiring a mechanism for restricting or retarding mixing. The increase in the viscosity of molten MgSiO$_3$ at lower mantle conditions is consistent with restricted convective mixing within the early magma ocean on Earth (see also Gurnis and Davies 1986; Garnero and McNamara 2008). Our results are suggestive although this issue is far from resolved; additional study is needed given our current lack of understanding of very high Rayleigh number magma ocean convective dynamics (e.g., Solomatov 2000).

Because the sign of $V_{\eta_1}^*$ is negative, the influence of pressure decreases at very high pressure. It would be worth investigating the viscosity at ultrahigh pressure (e.g., $P > 120$ GPa) in detail to see if an asymptote is approached or a maximum is attained. Simulations to evaluate these possibilities would have to be carried out along high-temperature isentropes (e.g., 5000–6000 K) because at lower temperature the computer glass transition intervenes (e.g., Morgan and Spera 2001).

APPLICABILITY OF STOKES-EINSTEIN AND EYRING RELATIONS

Because independent values for the self-diffusivity of Mg, O, and Si and the shear viscosity are available from the MD simulations, the applicability of the Stokes-Einstein and Eyring relations to molten MgSiO$_3$ can be addressed. These relations are often used to estimate shear viscosity from self-diffusion data (or vice versa) by assuming a characteristic particle (atom, molecule, or cluster) or activated complex "size." The problem however is in selecting the correct "size." Here, we invert the procedure and derive information regarding the size of the activated atom cluster involved in atom mobility and compare this with the structure of liquid MgSiO$_3$ inferred from coordination statistics. First we show the relationship between the Stokes-Einstein (SE) and Eyring models (EY) and then apply the generalized model to liquid MgSiO$_3$ using the MD simulation results to examine the size of the activated complex.

The SE relation relates the mobility of the diffusing unit (e.g., atom, molecule, or cluster) to the frictional force exerted on the unit as it moves through the surrounding medium of viscosity η. In the model, the hydrodynamic friction factor of a spherical "particle" (radius, a) is $f = 6\pi\eta a$ when no slip between the particle and continuum occurs or $f = 4\pi\eta a$ if a slip boundary condition is applied. The friction factor is related to the self-diffusion coefficient according to the Stokes-Einstein relation $f = kT/D$. Equating friction factors and rearranging gives a relationship between melt viscosity, self-diffusivity, and particle size:

$$6\pi a = \frac{kT}{D\eta} \qquad (6)$$

for no slip boundary condition and

$$4\pi a = \frac{kT}{D\eta} \qquad (7)$$

when slip conditions prevail.

The Eyring (1982) (EY) formulation is based on a somewhat more realistic atomic level picture. Diffusion of an atom (e.g., Mg, Si, or O) in the EY model occurs by a hop or a jump that results when the nearest neighbors defining a cluster surround-

ing the mobile atom undergoing diffusive motion are pushed aside. The EY relationship between self-diffusivity and viscosity (η) is

$$\xi (V/\mathrm{n N_A})^{1/3} = \frac{kT}{D\eta} \qquad (8)$$

where n is the number of atoms per formula unit (for MgSiO₃, n = 5) , V is the PT-dependent molar volume, N_A is Avogadro's number, and $\xi + 1$ is the number of atoms in the cluster, which we identify as the activated complex. The product on the right hand side of Equation 8 provides a characteristic linear dimension associated with the size of the "activated cluster" involved in the diffusion process in the EY model. Comparing Equations 6, 7, and 8, the SE and EY models are numerically equivalent provided $a = (V/\mathrm{nN_A})^{1/3}$ and the nearest neighbor coordination number ξ equals either $4\pi (\approx 12)$ or $6\pi (\approx 18)$ depending on applicable boundary conditions in the SE model.

In Figure 5, the quantity $\lambda = kT/D_O\eta$, which has the dimension of length, is plotted for oxygen at 4500 K. λ decreases as pressure increases from ~20 Å at low pressure to ca. 4 Å at 105 GPa. The rate of decrease of λ is greatest for $P < 30$ GPa and decreases at very high pressure (>90 GPa) where a decrease in the oxygen about oxygen mean coordination number drops from 15 to about 11 (Ghiorso et al. 2006). The SE model (slip conditions) has λ equal to $4\pi a$. Based on the SE model, values of $a \sim 1.5$ Å are found at low pressure, appropriate for oxygen that has an ionic radius of 1.38 Å. This simple picture breaks down, however, at higher pressure. At 60 GPa, for example, the SE radius of oxygen from Figure 5 is 0.6 Å, which is unrealistic. While the Stokes-Einstein analysis offers a glimpse into possible flow mechanisms, we conclude that its application to molten MgSiO₃ at high pressure is limited. In the Eyring model, the quotient $kT/D\eta$ equals $\xi(V/\mathrm{nN_A})^{1/3}$, the product of the number of nearest neighbors of the diffusing atom and mean particle size of the diffusing atom where $V = V(P,T)$ is the molar volume of liquid MgSiO₃ and n = 5 for MgSiO₃. The value of ξ is plotted on the right-hand side of Figure 5. The Eyring model indicates that the number of atoms ($\xi + 1$) in the activated complex relevant to shear flow decreases from ~8 atoms at low pressure to ~3 atoms at high pressure.

The SE has, as its underlying mechanism, the notion of a "particle" of radius a moving through a homogenous "fluid." While approximately reasonable at low pressure, the computed a rapidly approaches an unphysical value below 1 Å as pressure increases. In contrast, the Eyring model uses the notion of nearest neighbors in an activated complex and remains physically relevant throughout the entire pressure regime. By relying on the activated complex, we conclude that the Eyring model provides a more meaningful view of atom dynamics compared to the SE model for molten MgSiO₃. A more detailed picture of the correlation between the Eyring model ξ parameter and the local structure and dynamics of the melt at the atomic level must await a study of tagged particle dynamics at 10 fs resolution.

CONCLUDING REMARKS

Using molecular dynamics, we have examined the viscosity of molten MgSiO₃ using a pair-wise potential that compares favorably with FPMD studies and other pair-wise potentials. We
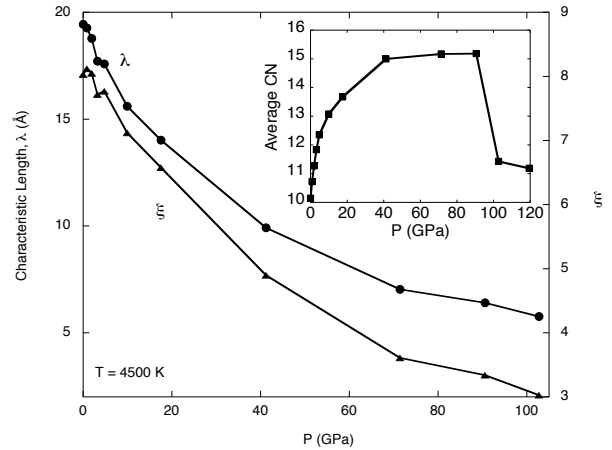

FIGURE 5. Characteristic length $\lambda = kT/D_O\eta$ for liquid MgSiO₃ plotted as a function of pressure for oxygen at 4500 K. In the Eyring model, λ is directly related to the number of atoms ($\xi + 1$) in the activated complex associated with shear viscous flow. ξ, the number of neighbors surrounding the mobile oxygen atom in the activated complex, is plotted on the right hand side of the figure.

have shown that there is a substantial increase in the viscosity of molten MgSiO₃ at high temperatures between 1 bar and 120 GPa (factors of 18 and 75 at 4500 and 3000 K, respectively). Along the isentrope, smaller viscosity increases of 2–6 (4000 and 2000 K, respectively) are found. This lends support for the idea of convective layering in the Hadean mantle. It has been suggested that this layering may have entrapped a complementary enriched reservoir. Further study is needed given the lack of understanding of very high Rayleigh number magma ocean convection. Finally, we have examined the Stokes-Einstein and Eyring models that relate atomic diffusion, shear viscosity and particle or cluster size and find that the Eyring model provides reasonable estimates for the size of the activated cluster involved in shear viscous flow across the wide range of pressures studied.

REFERENCES CITED

Akins, J.A., Luo, S.N., Asimow, P.D., and Ahrens, T.J. (2004) Shock-induced melting of MgSiO₃ perovskite and implications for melts in Earth's lowermost mantle. Geophysical Research Letters, 31, L14612.
Anderson, D.L. (2007) New Theory of the Earth: The dynamic planet radial and lateral structure sampling the Earth mineral physics origin and evolution of the layers and blobs energetics. Cambridge University Press, U.K.
Bennett, V.C., Brandon, A.D., and Nutman, A.P. (2007) Coupled ¹⁴²Nd-¹⁴³Nd isotopic evidence for Hadean mantle dynamics. Science, 318, 1907–1910.
Boyet, M. and Carlson, R.W. (2005) ¹⁴²Nd Evidence for early (>4.53 Ga) global differentiation of the silicate Earth. Science, 309, 576–581.
Eyring, H. (1982) Statistical Mechanics and Dynamics, 2nd edition, 785 p. Wiley, New York.
Garnero, E.J. and McNamara, A.K. (2008) Structure and dynamics of Earth's lower mantle. Science, 320, 626–628.
Gale, J.D. (1997) GULP: A computer program for the symmetry-adapted simula-

tion of solids. Journal of the Chemical Society, Faraday Transactions, 93, 629–37.

Ghiorso, M.S. (2004) An equation of state for silicate melts. III. Analysis of stoichiometric liquids at elevated pressure: Shock compression data, molecular dynamics simulations and mineral fusion curves. American Journal of Science, 304, 752–810.

Ghiorso, M.S., Nevins, D., and Spera, F.J. (2006) Molecular dynamics studies of MgSiO$_3$ liquid to 150 GPa: An equation of state (EOS), tracer diffusivities, and a detailed analysis of changes in atomic coordination statistics as a function of temperature and pressure. EOS Transactions AGU, 87, Fall Meeting Supplement, Abstract MR43B-1079.

Gurnis, M. and Davies, G.F. (1986) The effect of depth-dependent viscosity of convective mixing in the mantle and the possible survival of primitive mantle. Geophysical Research Letters, 13, 541–544.

Haile, J.M. (1992) Molecular Dynamics Simulation: Elementary Methods. Wiley, New York.

Hansen, J.P. and McDonald, I.R. (2006) Theory of Simple Liquids. Academic Press, New York.

Heinz, D.L. and Jeanloz, R. (1987) Measurement of the melting curve of Mg$_{0.9}$Fe$_{0.1}$SiO$_3$ at lower mantle conditions and its geophysical implications. Journal of Geophysical Research: Solid Earth, 92, 11437–11444.

Ito, E. and Katsura, T. (1992) Melting of ferromagnesian silicate perovskite under lower mantle conditions. In Y. Syono and M.H. Manghani, Eds., High Pressure Research in Mineral Physics: Applications to Earth and Planetary Sciences, p. 35–44. Terra Scientific, Tokyo.

Knittle, E. and Jeanloz, R. (1989) Melting curve of (Mg,Fe)SiO$_3$ perovskite to 96 GPa: Evidence for a structural transition in lower mantle melts. Geophysical Research Letters, 16, 421–424.

Kubicki, J.D. and Lasaga, A.C. (1991) Molecular dynamics simulations of pressure and temperature effects on MgSiO$_3$ and Mg$_2$SiO$_4$ melts and glasses. Physics and Chemistry of Minerals, 17, 661–673.

Lacks, D.J., Rear, D.B., and Van Orman, J.A. (2007) Molecular dynamics investigation of viscosity, chemical diffusivities and partial molar volumes of liquids along the MgO-SiO$_2$ join as functions of pressure. Geochimica et Cosmochimica Acta, 71, 1312–1323.

Lay, T., Garnero, E.J., and Williams, Q. (2004) Partial melting in a thermo-chemical boundary layer at the base of the mantle. Physics of the Earth and Planetary Interiors, 146, 441–467.

Morgan, N.A. and Spera, F.J. (2001) The glass transition, structural relaxation and theories of viscosity: A molecular dynamics study of amorphous CaAl$_2$Si$_2$O$_8$. Geochimica et Cosmochimica Acta, 65, 4019–4041.

Nevins, D. (2009) Understanding silicate geoliquids at high temperatures and pressures through molecular dynamics simulations. Ph.D. thesis, University of California, Santa Barbara.

Nevins, D. and Spera, F.J. (2007) Accurate computation of shear viscosity from equilibrium molecular dynamics simulations. Molecular Simulation, 33, 1261–1266, DOI: 10.1080/08927020701675622.

Oganov, A.R., Brodholt, J.P., and Price, G.D. (2000) Comparative study of quasiharmonic lattice dynamics, molecular dynamics, and Debye model applied to MgSiO$_3$ perovskite. Physics of the Earth and Planetary Interiors, 122, 277–288.

Plimpton, S. (1995) Fast parallel algorithms for short-range molecular dynamics. Journal of Computational Physics, 117, 1–19.

Refson, K. (2001) Moldy User's Manual. Department of Earth Sciences, University of Oxford.

Shen, G.Y. and Lazor, P. (1995) Measurement of melting temperatures of some minerals under lower mantle pressures. Journal of Geophysical Research: Solid Earth, 100, 17699.

Solomatov, V.S. (2000) Fluid dynamics of a terrestrial magma ocean. In R. Canup and K. Righter, Eds., Origin of the Earth and Moon, p. 323–338. University of Arizona Press, Tucson.

Speziale, S., Zha, C.-S., Duffy, T.S., Hemley, R.J., and Mao, H.-K. (2001) Quasi-hydrostatic compression of magnesium oxide to 52 GPa: Implications for the pressure-volume-temperature equation of state. Journal of Geophysical Research, 106, 515–528.

Stixrude, L. and Karki, B. (2005) Structure and freezing of MgSiO$_3$ liquid in Earth's lower mantle. Science, 310, 297–299, DOI:10.1126/science.1116952.

Sweeney, J.S. and Heinz, D.L. (1993) Melting of iron-magnesium-silicate perovskite. Geophysical Research Letters, 20, 855–858.

Valencia, D., Sasselov, D.D., and O'Connell, R.J. (2007) Radius and structure models of the first super-Earth planet. The Astrophysical Journal, 656, 545–551, DOI: 10.1086/509800.

van Beest, B.W.H., Kramer, G.J., and van Santen, R.A. (1990) Force fields for silicas and aluminophosphates based on ab initio calculations. Physical Review Letters, 64, 1955–1958.

Wan, J.T.K., Duffy, T.S., Scandolo, S., and Car, R. (2007) First-principles study of density, viscosity, and diffusion coefficients of liquid MgSiO$_3$ at conditions of the Earth's deep mantle. Journal of Geophysical Research, 112, B03208, DOI: 10.1029/2005JB004135.

Zerr, A., Diegeler, A., and Boehler, R. (1998) Solidus of Earth's deep mantle. Science, 281, 243–246, DOI: 10.1126/science.281.5374.243.

Zwanzig, R. (1983) On the relation between self-diffusion and viscosity of liquids. Journal of Chemical Physics, 79, 4507–4508, DOI: 10.1063/1.446338.